Supplementary data for:

Mechanism and modeling of hexavalent chromium interaction with a typical black soil: the importance of the relationship between adsorption and reduction

Jia Zhang[1], Huilin Yin[1,2], Samuel Barnie[1], Minghai Wei[1,2*], Honghan Chen[1]

1   Beijing Key Laboratory of Water Resources & Environmental Engineering, China University of Geosciences, Beijing 100083, China

2   Chinese Academy for Environmental Planning

——**Submit to *RSC Advances***

Corresponding author:

Minghai Wei

Beijing Key laboratory of Water Resources and Environmental Engineering, China University of Geosciences, Beijing 100083, P. R. China

E-mail: wmh87@163.com

Summary:

22 Pages

17 Figures

3 Tables

1 text

Two-step kinetic model development processes

(1) Conceptual model

According to the "adsorption-reduction" mechanism of Cr(VI) retention by the black soil, a corresponding conceptual model was established, and the Cr(VI) retention processes can be divided into two steps: (1) Cr(VI) is adsorbed onto the surface of black soil particle by electrostatic attraction force; (2) the adsorbed Cr(VI) is sequentially reduced into Cr(III) by electron donors on soil particles, such as soil organic matters.

(2) Mathematical model

First step:

Cr(VI) adsorption from liquid phase onto solid phase, is mainly governed by the concentration difference between bulk solution and solid phase, which can be described by classical Fick first diffusion law.

$$\frac{dC_t}{dt} = -k_1(C_t - C_e)$$

Eq. S1

where, C_t and C_e respectively represent real-time and equilibrium Cr(VI) concentration in bulk solution. k_1 is the adsorption rate constant.

In traditional adsorption models, the concentration distribution ratio of Cr(VI) in the liquid and solid phase can be expressed as distribution coefficient K_d, which is the function of temperature. As in this two-step kinetic model the adsorbed Cr(VI) can be further reduced, the C_e is no longer a constant, which turns to be a function of Cr(VI) concentration on solid phase. The function is shown as follow.

$$C_e = \frac{q_s}{K_d}$$

Eq. S2

where, q_s represents Cr(VI) concentration in diffuse layer. Based on Eq. S2, the Eq. S1 can be corrected as follow.

$$\frac{dC_t}{dt} = -k_1\left(C_t - \frac{q_s}{K_d}\right)$$

Eq. S3

Second step:

In this step, the adsorbed Cr(VI) is reduced into Cr(III), which is a typical

chemical reaction process between Cr(VI) and electron donors on soil particles, and this reaction can be described by classical first-order kinetic model. Additionally, considering that the adsorption of Cr(VI) from bulk solution acts as a source of adsorbed Cr(VI), the reaction can be expressed as the following form.

$$\frac{dq_s}{dt} = -k_2 q_s + \frac{V}{m} k_1 \left(C_t - \frac{q_s}{K_d} \right)$$

Eq. S4

where, k_2 represents the reduction rate constant. The C_t and q_s represent Cr(VI) concentration in liquid and solid phase respectively, so they have different units, and thus a unit conversion is needed. V represents the volume of bulk solution, and m is the mass of the soil sample.

According to the conceptual model, Cr(VI) reduction on soil particle is the single source of the reduced Cr(III), and thus the reduced Cr(III) can be expressed as the following equation.

$$\frac{dq_{re}}{dt} = k_2 q_s$$

Eq. S5
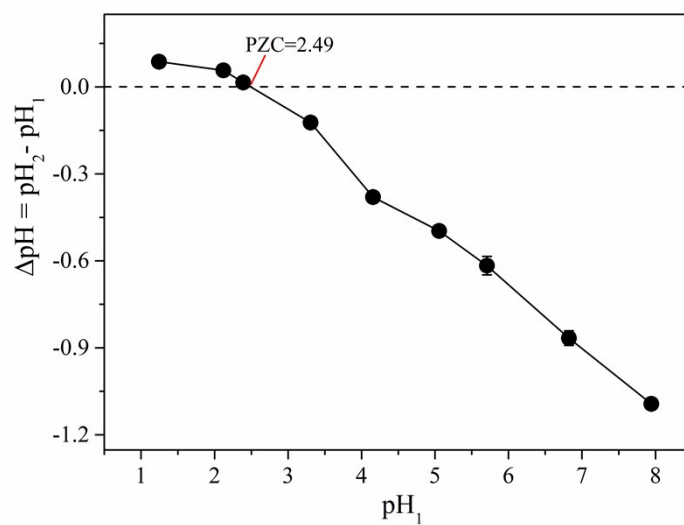
Fig. S1 The ZPC determination curve according to the method described elsewhere (Lu et. al., 2006).
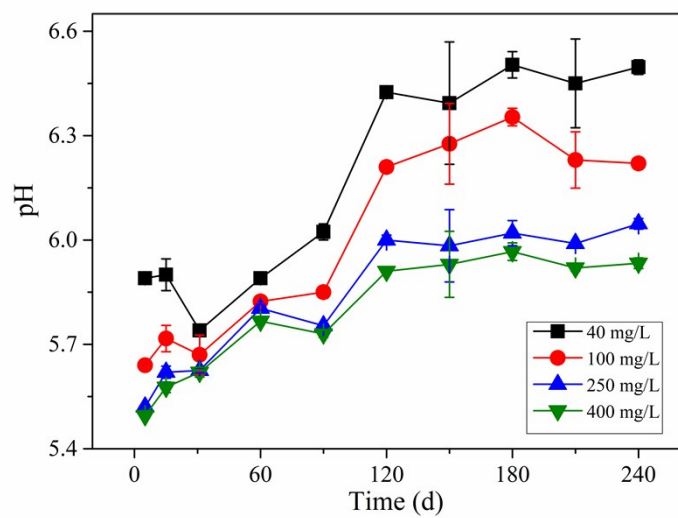
Fig. S2 The pH variation with time under different initial Cr(VI) concentrations under pH 5.7.
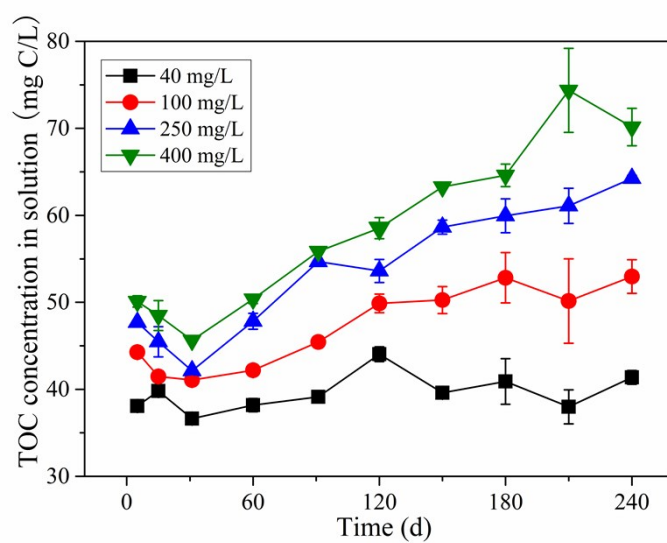
Fig. S3 The TOC concentration variation in solution with time under different initial Cr(VI) concentrations under pH 5.7.
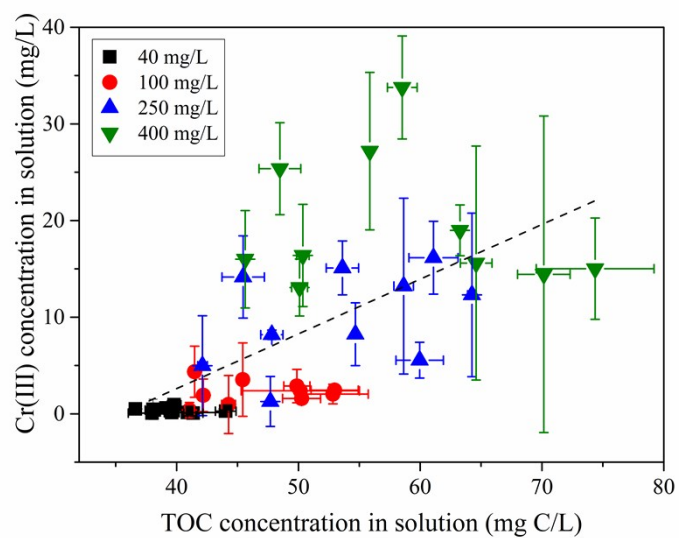
Fig. S4 The correlation between Cr(III) concentration in solution and TOC concentration in solution under different initial Cr(VI) concentrations.
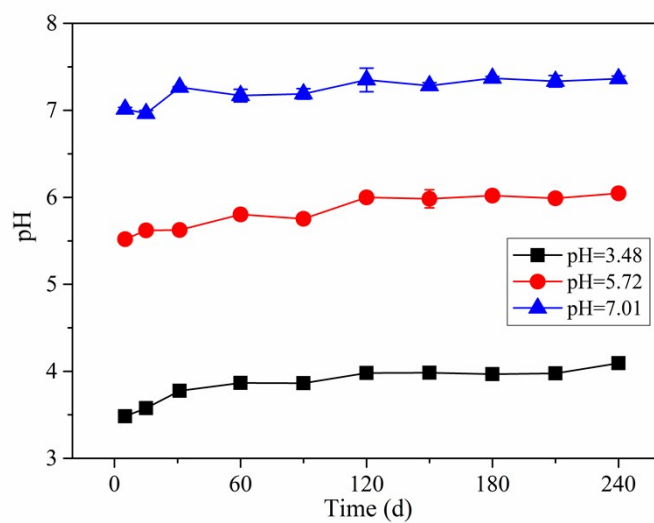
Fig. S5 The pH variation in solution with time under different initial pH conditions under initial Cr(VI) concentration of 250 mg/l.
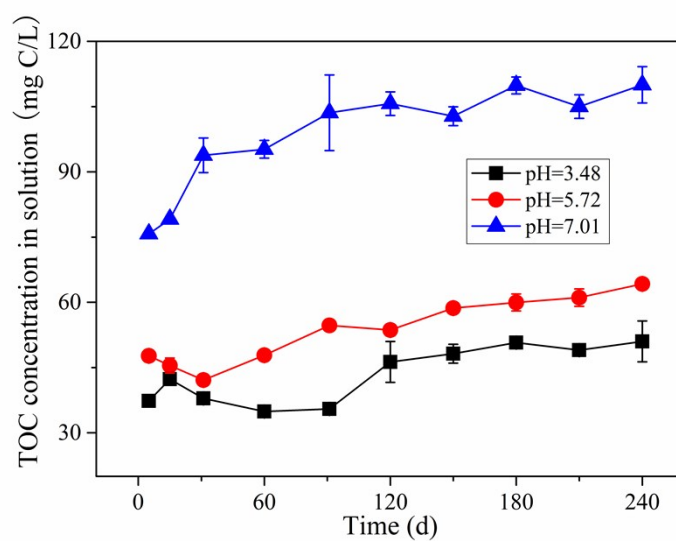
Fig. S6 The TOC concentration variation in solution with time under different initial pH conditions under initial Cr(VI) concentration of 250 mg/l.
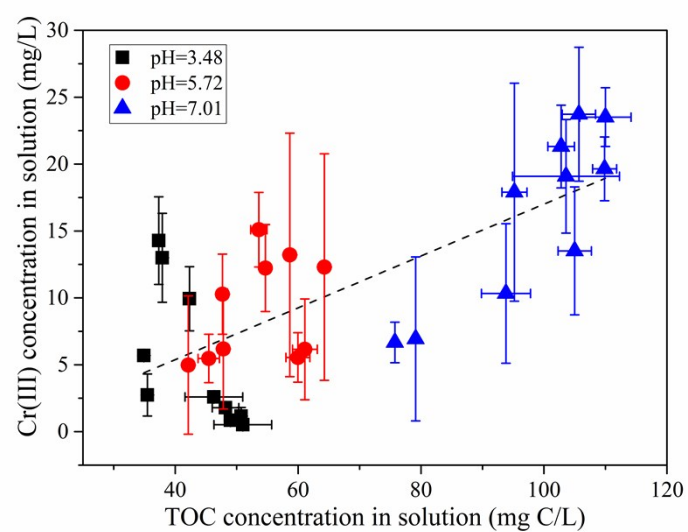
Fig. S7 The correlation between Cr(III) concentration in solution and TOC concentration in solution under different initial pH conditions.

Table S1 The fitting parameters of kinetic data under different initial Cr(VI) concentrations by linear and Freundlich isotherm models.

Linear isotherm model			Freundlich isotherm model		
$q_s=K_d{\cdot}C_t+q_0$			$q_s=K_F{\cdot}C_t^{1/n}$		
K_d (L/g)	q_0 (mg/g)	R^2	K_F	n	R^2
0.0017	0.0270	0.9842	0.0067	1.3308	0.9919

Table S2 The fitting parameters of kinetic data under different initial pH conditions by linear and Freundlich models.

| Initial pH | Linear isotherm model | | | Freundlich isotherm model | | |
| | $q_s = K_d \cdot C_t + q_0$ | | | $q_s = K_F \cdot C_t^{1/n}$ | | |
	K_d (L/g)	q_0 (mg/g)	R^2	K_F	n	R^2
3.5	0.0068	0.2327	0.9078	0.2108	6.4719	0.9535
5.7	0.0018	0.0274	0.9002	0.0067	1.3308	0.9919
7.0	0.0010	-0.0289	0.8550	0.0004	0.8540	0.8523
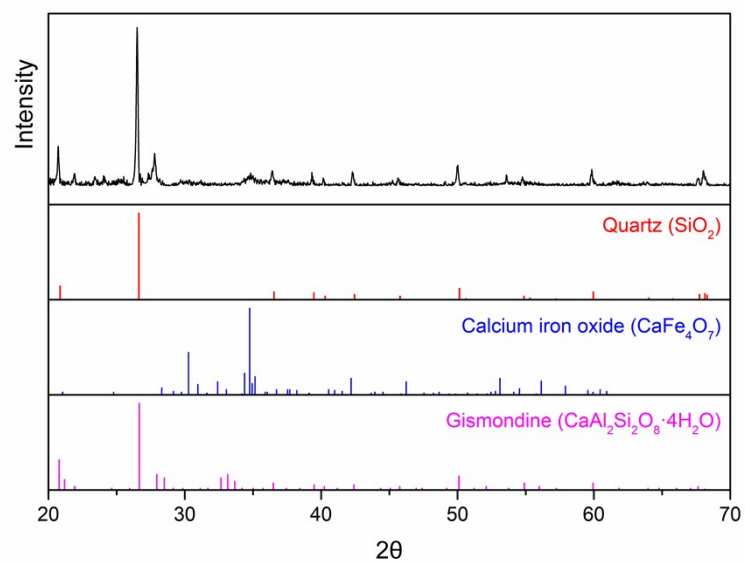
Fig. S8 The XRD pattern of the black soil sample used in this experiment.
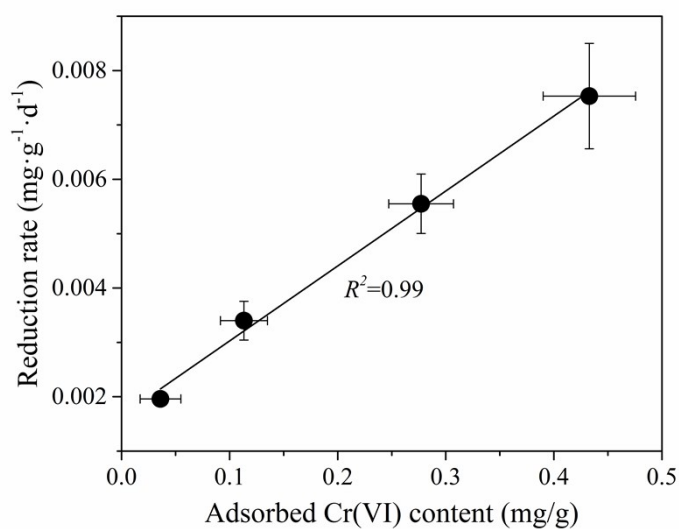
Fig. S9 The correlation between adsorbed Cr(VI) content on soil particles and Cr(VI) reduction rate in the system under different initial Cr(VI) concentrations of 40, 100, 250 and 400 mg/l under pH 5.7. The adsorbed Cr(VI) content was determined by the average value of the adsorbed Cr(VI) contents ranging from 5 to 120 d. The horizontal error bar was the standard deviation of the adsorbed Cr(VI) contents. The Cr(VI) reduction rate was determined by the slope of linear fitting result of Cr(III) content variation in the system ranging from 5 to 120 d. The vertical error bar was the uncertainty of the linear fitting.
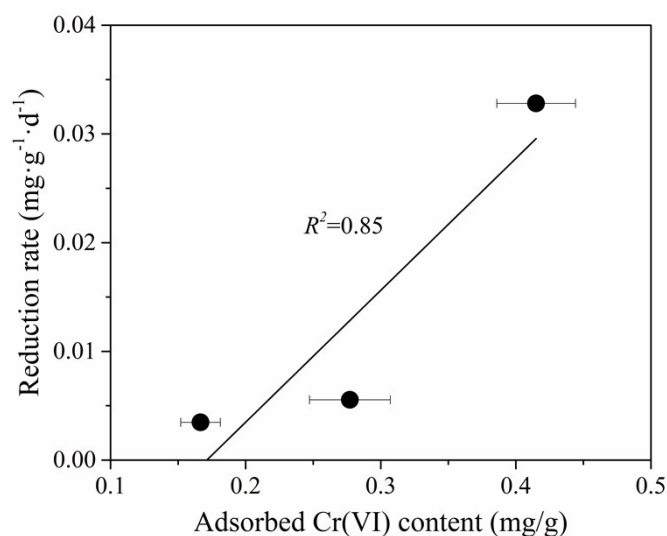
Fig. S10 The correlation between adsorbed Cr(VI) content on soil particles and Cr(VI) reduction rate in the system under different pH conditions of 3.5, 5.7 and 7.0under initial Cr(VI) concentration of 250 mg/l. The adsorbed Cr(VI) content under the pH 5.7 and 7.0 was determined by the average value of the adsorbed Cr(VI) contents ranging from 5 to 120 d, and Cr(VI) content under the pH 3.5 was determined by the average value of the adsorbed Cr(VI) contents ranging from 5 to 30 d. The horizontal error bar was the standard deviation of the adsorbed Cr(VI) contents. The Cr(VI) reduction rate was determined by the slope of linear fitting result of Cr(III) content variation in the system ranging from 5 to 120 d. The vertical error bar was the uncertainty of the linear fitting.
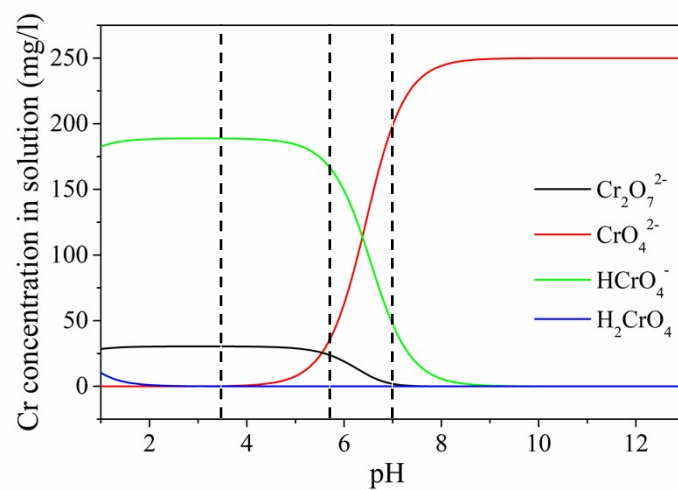
Fig. S11 The Cr(VI) anion species variation with pH from 1 to 13. The result was simulated by the Visual Minteq 3.1 software. The initial concentration of Cr(VI) was set as 250 mg/l, and the temperature was set as 25 °C.
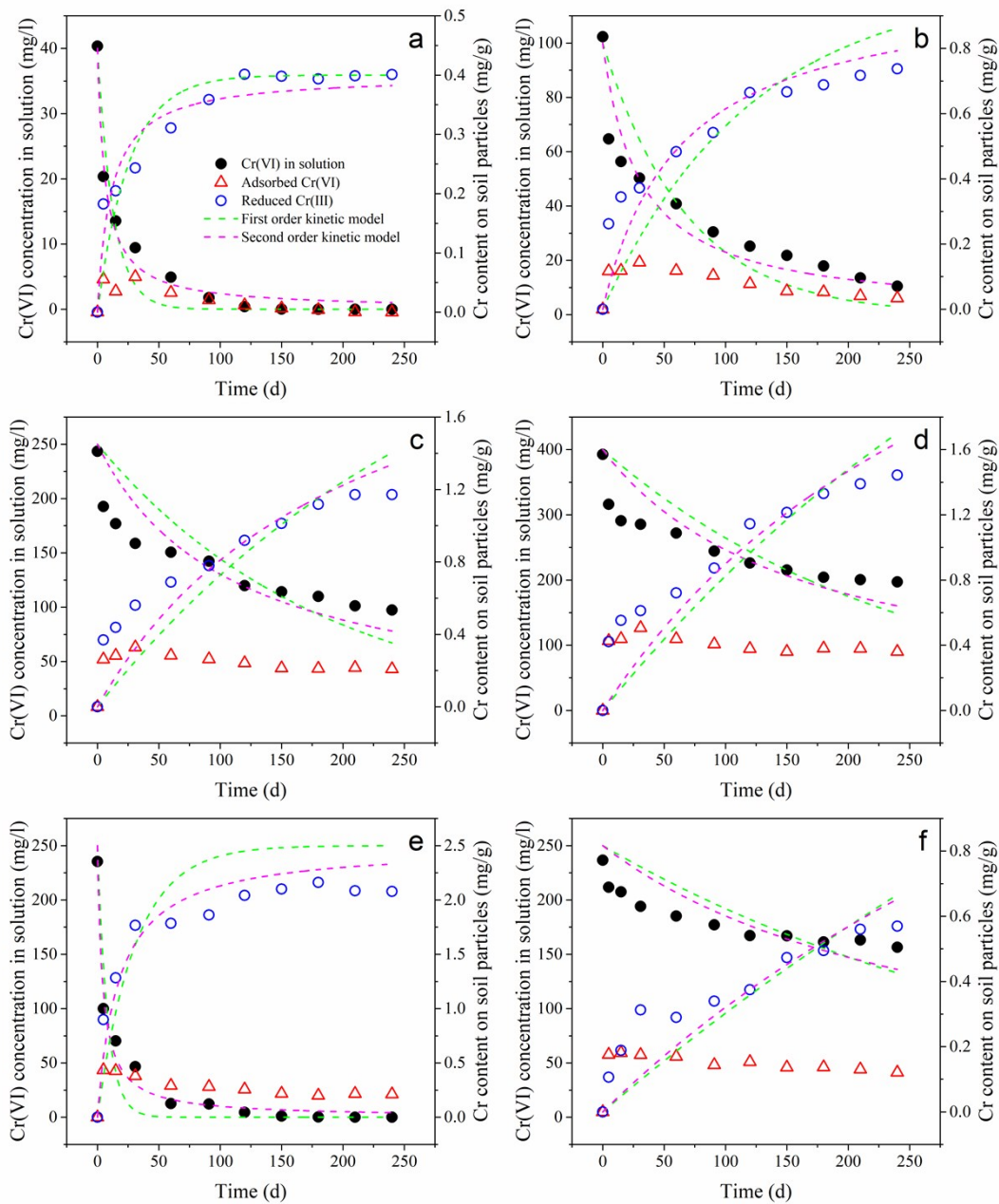
Fig. S12 The time evolution of Cr(VI) concentration in solution, adsorbed Cr(VI) content and reduced Cr(III) content under different initial Cr(VI) concentration and pH conditions. The curves are the fitting results of the first and second order kinetic models. (a-d) represent the fitting results of initial Cr(VI) concentration ranging from 40 to 400 mg/l under pH 5.7. (e) and (f) represent the fitting results of initial pH 3.5 and 7.0 under initial Cr(VI) concentration of 250 mg/l.

Table S3 Optimized parameters of the first and second order kinetic models for the remaining Cr(VI) concentration in solution and reduced Cr(III) content in the reaction system under different initial Cr(VI) concentrations and pH conditions.

| Condition | Cr(VI) concentration (mg/l) | pH | First order kinetic model | | | | Second order kinetic model | | | |
| | | | Cr(VI) in solution | | Reduced Cr(III) | | Cr(VI) in solution | | Reduced Cr(III) | |
			k	R^2	k	R^2	k	R^2	k	R^2
a	40	5.7	0.07674	0.9343	0.00392	0.9842	0.03864	0.8923	0.00225	0.939
b	100	5.7	0.0147	0.7329	0.0083	0.686	0.0003	0.9063	0.0002	0.8654
c	250	5.7	0.0055	0.4588	0.0034	0.6973	0.00004	0.6822	0.00002	0.8046
d	400	5.7	0.0041	0.3432	0.0023	0.7196	0.00002	0.5544	0.00001	0.7921
e	250	3.5	0.1199	0.9144	0.0326	0.6519	0.0009	0.9791	0.0002	0.9095
f	250	7.0	0.0026	0.0511	0.00129	0.7047	0.00001	0.02662	0.00001	0.7487
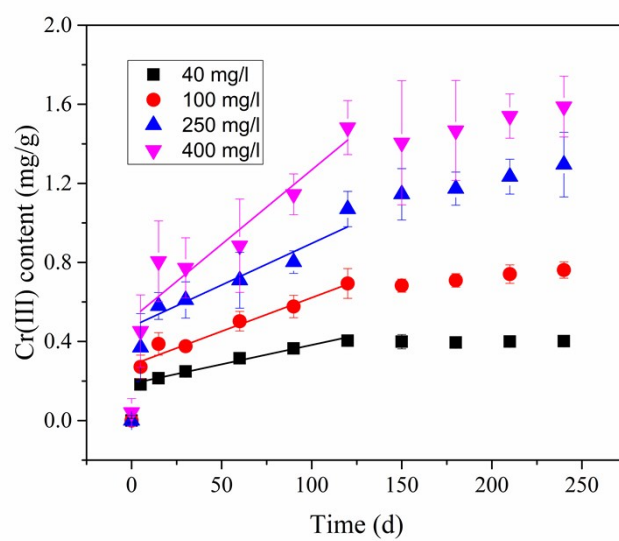
Fig. S13 The linear fitting of the reduced Cr(III) content variation with time under different initial Cr(VI) concentration.
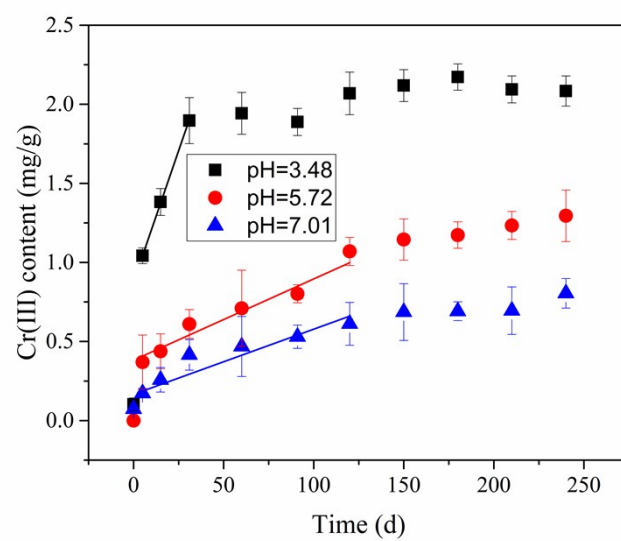
Fig. S14 The linear fitting of reduced Cr(III) content variation with time under different initial pH conditions.
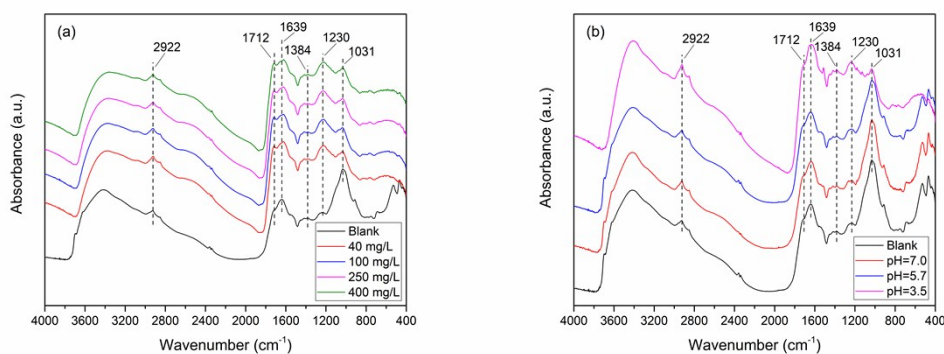
Fig. S15 The FTIR spectra of HA samples extracted from the soil samples after reacting with Cr(VI) under different (a) initial Cr(VI) concentration and (b) pH conditions for 240 d. The blank represent the blank control group, where the soil samples were shaken in the solution without Cr(VI) under the same experimental condition for 240 d.
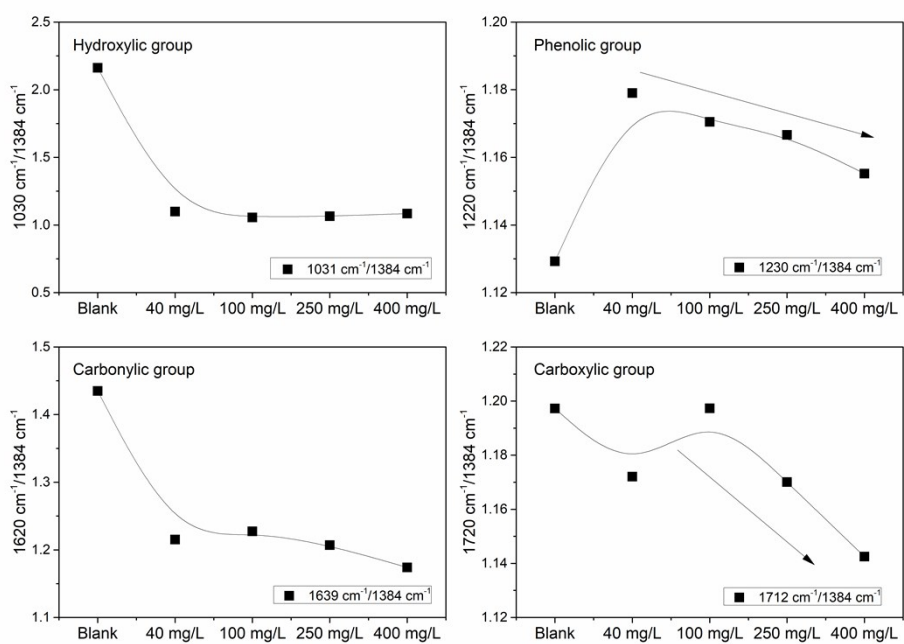
Fig. S16 The absorbance band intensity ratio of hydroxyl (1031 cm^{-1}), phenol (1230 cm^{-1}), carbonyl (1639 cm^{-1}) and carboxyl (1712 cm^{-1}) to methyl (1384 cm^{-1}) of HA samples extracted from the soil samples reacted with Cr(VI) under different initial Cr(VI) concentrations for 240 d.
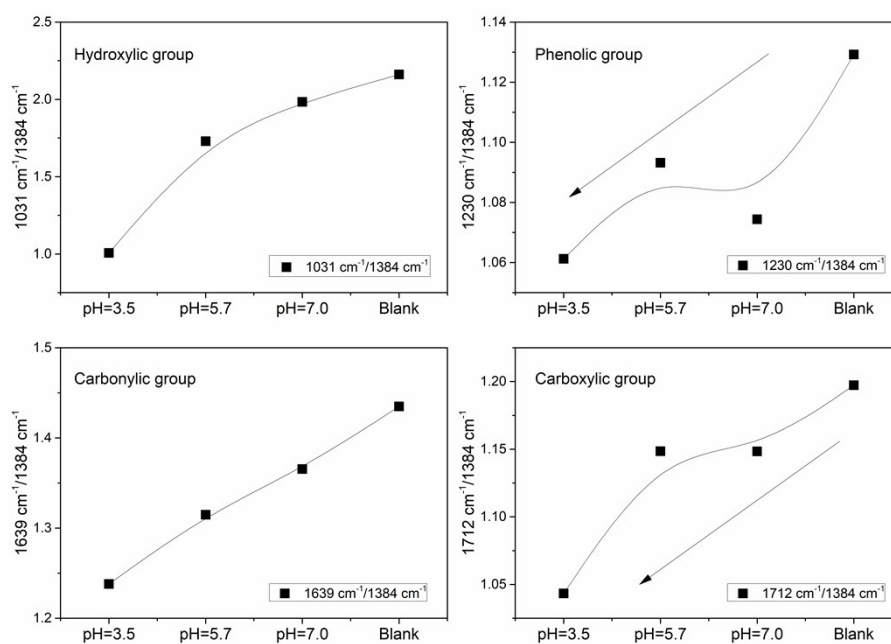
Fig. S17 The absorbance band intensity ratio of hydroxyl (1031 cm^{-1}), phenol (1230 cm^{-1}), carbonyl (1639 cm^{-1}) and carboxyl (1712 cm^{-1}) to methyl (1384 cm^{-1}) of HA samples extracted from the soil samples reacted with Cr(VI) under different pH conditions for 240 d.